Mineralogical Magazine, April 2004, Vol. 68(2), pp. 353–368

Dedicated to the memory of Dr A. J. Criddle, Natural History Museum, London, who died in May 2002

Origin of placer laurite from Borneo: Se and As contents, and S isotopic compositions

K. H. HATTORI[1,*], L. J. CABRI[2], B. JOHANSON[3] AND M. L. ZIENTEK[4]

[1] University of Ottawa, Ottawa, Canada
[2] 99 Fifth Avenue, Suite 122, Ottawa, Canada
[3] Geological Survey of Finland, Espoo, Finland
[4] US Geological Survey, Spokane, USA

ABSTRACT

We examined grains of the platinum-group mineral, laurite (RuS_2), from the type locality, Pontyn River, Tanah Laut, Borneo, and from the Tambanio River, southeast Borneo. The grains show a variety of morphologies, including euhedral grains with conchoidal fractures and pits, and spherical grains with no crystal faces, probably because of abrasion. Inclusions are rare, but one grain contains Ca-Al amphibole inclusions, and another contains an inclusion of chalcopyrite+bornite+pentlandite+heazlewoodite (Ni_3S_2) that is considered to have formed by a two-stage process of exsolution and crystallization from a once homogeneous Fe-Cu-Ni sulphide melt.

All grains examined are solid solutions of Ru and Os with Ir (2.71–11.76 wt.%) and Pd (0.31–0.66 wt.%). Their compositions are similar to laurite from ophiolitic rocks. The compositions show broad negative correlations between Os and Ir, between As and Ir, and between As (0.4–0.74 wt.%) and Se (140 to 240 ppm). Laurite with higher Os contains more Se and less Ir and As. The negative correlations between Se and As may be attributed to their occupancy of the S site, but the compositional variations of Os, Ir and As probably reflect the compositional variation of rocks where the crystals grew.

Ratios of S/Se in laurite show a narrow spread from 1380 to 2300, which are similar to ratios for sulphides from the refractory sub-arc mantle. Sulphur isotopic compositions of laurite are independent of chemical compositions and morphologies and are similar to the chondritic value of 0‰. The data suggest that S in laurite has not undergone redox changes and originated from the refractory mantle. The data support the formation of laurite in the residual mantle or in a magma generated from such a refractory mantle, followed by erosion after the obduction of the host ultramafic rocks.

KEYWORDS: PGM, nugget, alluvial placer, placer deposit, electron-microprobe, stable-isotopes, osmium, SEM data, Kalimantan, trace-element geochemistry.

Introduction

COARSE-GRAINED platinum-group minerals (PGM) have been recovered from many placers associated with ultramafic-mafic igneous rocks. The view of their origin prevailing before the mid-1980s was that they crystallized in magmas and then were mechanically eroded from the igneous rocks (Cabri and Harris, 1975; Slansky *et al.*, 1991; Cabri *et al.*, 1996). The rare occurrences of coarse-grained PGM in igneous rocks led to the suggestion that they formed in late magmatic-pegmatitic environments (Johan *et al.*, 2000), as well as low-temperature crystallization of PGM during the weathering of mafic rocks (Augustithis, 1965; Ottemann and Augustithis, 1967; Cousins, 1973; Cousins and Kinloch, 1976; Stumpfl, 1974), and during sedimentation in placers (Barker and Lamal, 1989; Bowles, 1986, 1988; Bowles *et al.*, 2000).

* E-mail: khattori@uottawa.ca
DOI: 10.1180/0026461046820192

Osmium isotopic data have contributed to the discussion. A relatively narrow spread of $^{187}Os/^{188}Os$ is used to support the mechanical derivation of PGM from Alpine-type and Alaskan-type intrusions (Hattori and Cabri, 1992; Cabri *et al.*, 1996), and a considerable isotopic variation from PGM associated with large intrusions, such as those in Freetown Complex (Hattori *et al.*, 1991), is explained by the isotopic heterogeneity of host igneous rocks (Hattori, 2002). However, in contrast, Bowles *et al.* (2000) attributed the variation of $^{187}Os/^{188}Os$ in PGM associated with the Freetown Complex to surface processes and crystallization of PGM in placers. Bird *et al.* (1999) found elevated concentrations of ^{186}Os in leachates during acid extractions of Os from placer PGM associated with Josephine ophiolite, Oregon, and suggested their crystallization near the core-mantle boundary. In contrast, Meibom *et al.* (2002) attributed the variation of ^{186}Os to heterogeneity of the upper mantle.

In order to constrain the origin of coarse-grained PGM, we determined the concentrations of As and Se and the S isotopic compositions, because these values are susceptible to hydrothermal and low-temperature processes.

Sample locations

The laurite grains examined in this study are from the Tanah Laut subprovince, in the province of South Kalimantan, Indonesia (Fig. 1*a*). The grains were collected from placer deposits at the type locality (BM40504) from the Pontyn (Pontijn) River (sample numbers starting with P) near the town of Asemasen on the southeast coast of Borneo and from the Tambanio River (sample number starting with T), upstream of the village of Riampinang (~3° 40′S and 114° 55′ E), also in the southeastern Borneo (Fig. 1*a*,*b*).

The laurite samples from Pontyn were donated to the Natural History Museum, London, by Dr Phoebus in 1866 together with native platinum, Fe-Pt alloys, gold, cinnabar and hydrocerussite $Pb_3(CO_3)_2(OH)_2$. E. Wöhler at Göttingen identified laurite as a new mineral in the same year (Wöhler, 1866). We confirmed the identity of laurite and the last two minerals using X-ray diffraction (XRD).

At the Tambanio locality, the laurite grains were collected from sediments in the main channel of the river, upstream from the junction with the westward-flowing Buluhembok River (Fig. 1*a*,*b*). No other PGM were recovered at this site. Metasedimentary and metavolcanic rocks, tonalitic gneiss, and schist occur in the watershed immediately upstream of the laurite occurrence (Zientek and Page, 1990), but small northwest-flowing tributaries drain from ophiolite complexes of the Meratus Range to the site. The laurite is believed to have been derived from the ophiolitic rocks. The laurite locality is ~4 km upstream from the gold-PGE placers and lode occurrences described by Zientek *et al.* (1992). Burgath and Mohr (1986) and Burgath (1988) described the PGM-bearing ophiolites in the area.

Hattori *et al.* (1992) reported the occurrence of laurite grains and their Os isotopic compositions in chromitites of the Meratus Range ophiolite at Sungai Kalaan and compared the data with placer laurite grains collected from the streams draining from these ophiolitic rocks in the same area.

Analytical procedure

The Pontyn River laurite grains were selected using a binocular microscope. Laurite grains are black with a metallic blue tinge. After cleaning the samples in detergent water in an ultrasonic bath for >20 min, the morphology of mineral grains was examined using a JEOL 6400 digital scanning electron microscope (SEM) equipped with a LINK EXL energy-dispersive X-ray analyser. The operating conditions were 20 kV, accelerating voltage and 0.5 nA beam current. The major element compositions were determined on the grains coated with carbon, using a Cameca Camebax MBX electron microprobe equipped with four wavelength dispersive spectrometers. The analytical conditions were 20 kV accelerating voltage and 35 nA beam current using Os-$L\beta$, Ir-$L\alpha$, Ru-$L\alpha$, Rh-$L\alpha$, Pt-$L\alpha$, Pd-$L\beta$, As-$L\beta$, Ni-$K\alpha$. Standards are pure metals and alloys except for a pyrite standard for S-$K\alpha$. Raw X-ray data were converted to wt.% using the Cameca PAP matrix correction program.

Minor element concentrations were determined using a Cameca SX 50 equipped with four wavelength-energy dispersive spectrometers. Se-$L\alpha$ on TAP As-$K\beta$ on LiF. As-$K\alpha$ was used for base metal sulphides, but not used for laurite because of overlaps with Os-$L\beta_2$. Instead, As-$K\beta$ was measured with LiF. Analytical conditions were 35 kV and beam current of 500 nA. Measuring time was 300 s for peak and 300 s for backgrounds. The minimum detection limits are defined as $3\sqrt{B} \times \sqrt{t}$, where B is background

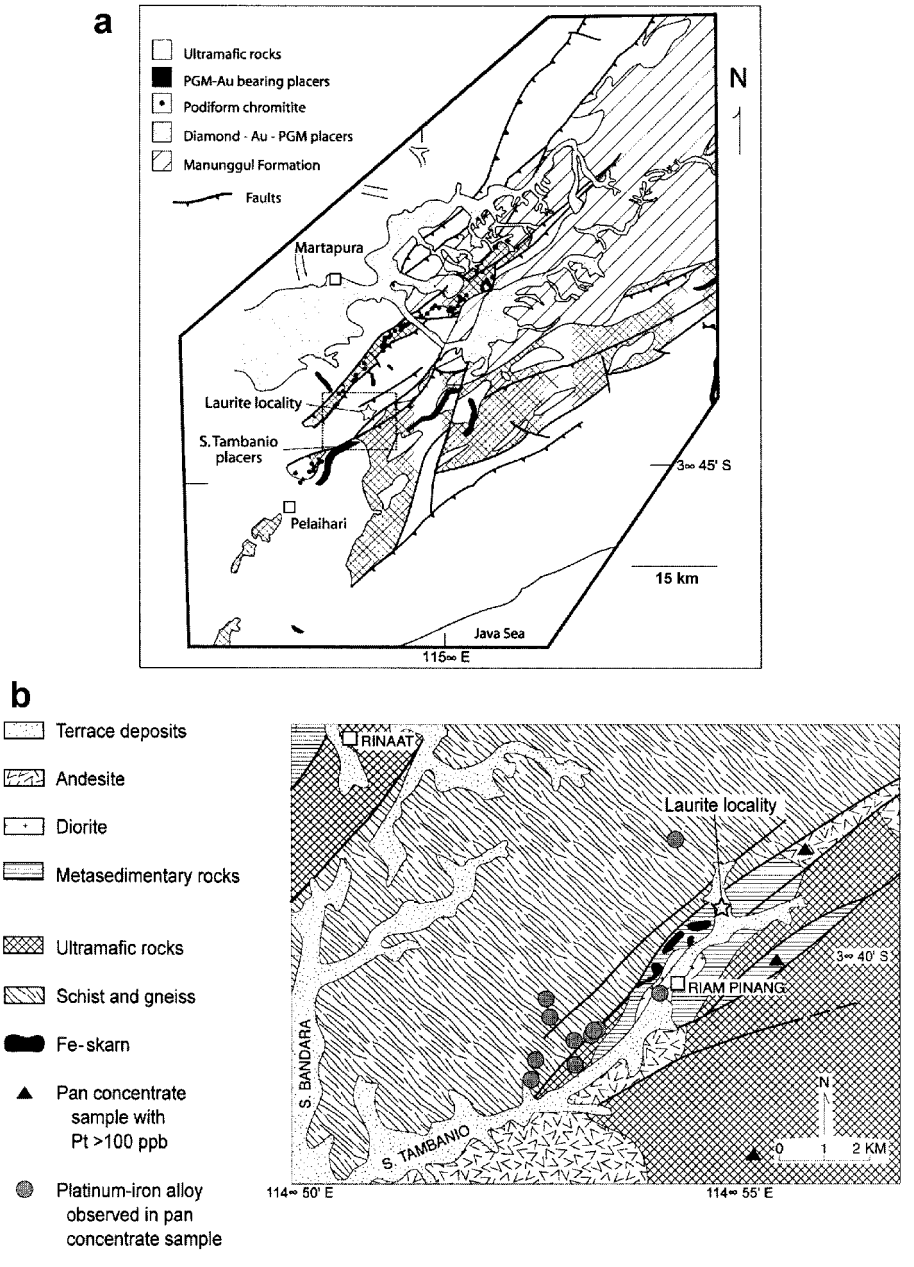

FIG. 1. (*a*) Map showing the laurite sample locality (open star), towns and villages (open squares) and selected features relevant to the placer PGM occurrences in southeastern Kalimantan. They include diamond-Au-PGM placers (dotted areas), PGM-Au placers (solid colour), podiform chromitite deposits (solid circles), ultramafic rocks (hatched pattern), and the Manunggul Formation (inclined stripe). The detailed geology of the dotted rectangular area close to the laurite location is shown in Fig. 1*b*. The Late Cretaceous sedimentary and mafic volcanic rocks of the Manunggul Formation appear to be the source of the diamond-bearing placers. Modified from Zientek *et al*. (1992). (*b*) Geological map of the Riam Pinang area, South Kalimantan. The location of the laurite samples is shown relative to the native gold-platinum-iron alloy-bearing placers downstream from Riam Pinang (area with PGM observed in pan concentrate samples). Modified from Zientek *et al*. (1992).

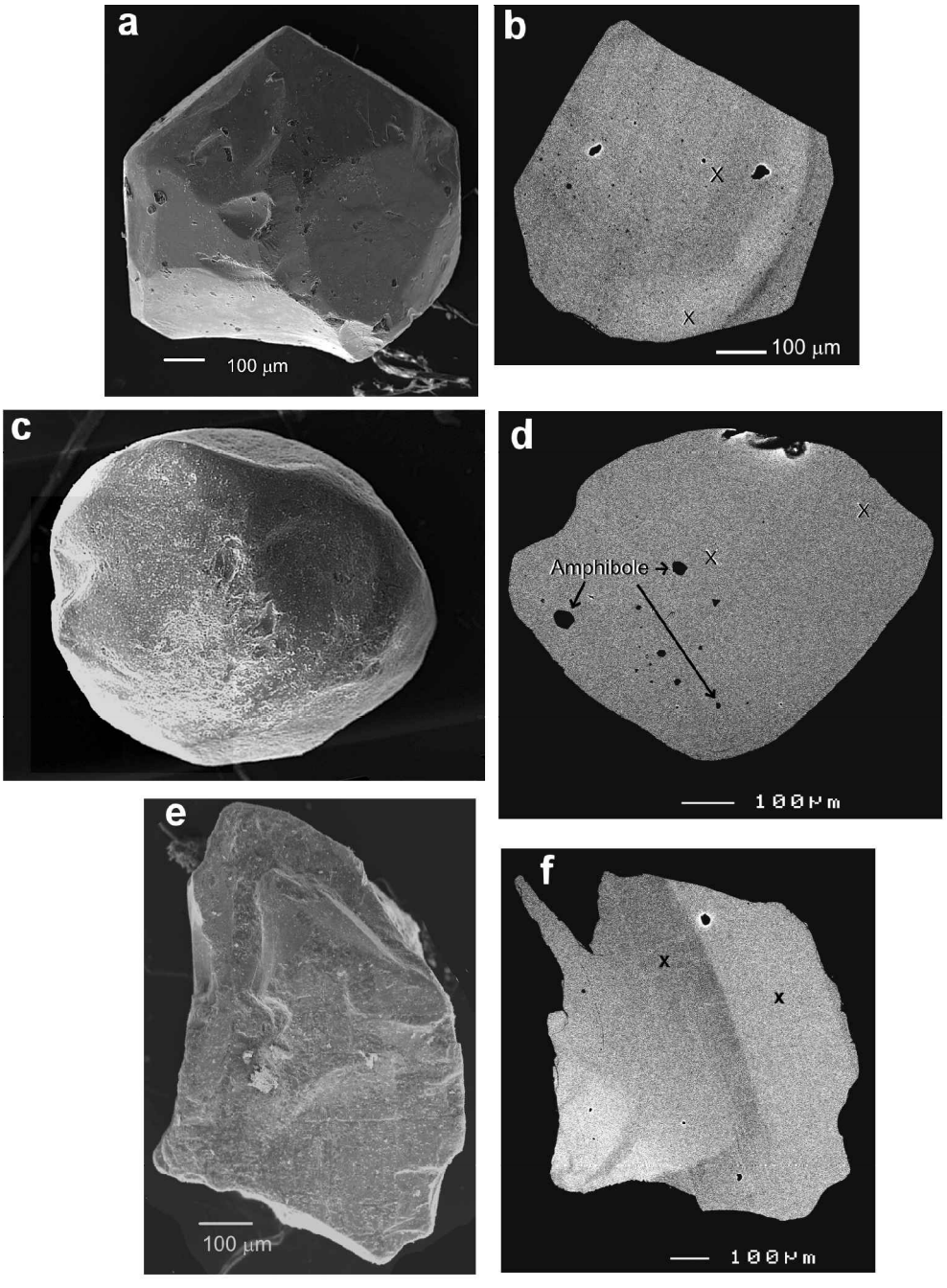

FIG. 2. Morphology and BSE images of selected laurite grains. X marks the areas chosen for the analyses. Scale bars are all 100 μm. The brighter areas correspond to higher Os and the darker areas to higher Ru contents. (*a*) Morphology of grain P-1-1.; (*b*) BSE image of the grain, P-1-1; (*c*) spherical shape of P-2-6; (*d*) BSE image of the grain, P-2-6, with several inclusions of amphiboles; (*e*) angular shape with abundant fractures of P-2-9; and (*f*) BSE image of the grain P-2-9.

count on either side of the peak and *t* the counting time. Under the analytical conditions above, the detection limits for Se are 15 ppm for laurite and 8 ppm for other sulphides, those for As are 370 ppm for laurite and 30 ppm for other sulphides. The proximity of Os-$K\beta$ to the As-$L\beta_2$ line and of the Os-$L\beta_8$ line to the Se-$L\alpha$ line raised the detection limit of As and Se in laurite. Standards used are pure metallic Se and cobaltite for As (45.2 wt.% As). Replicate analyses of 12 spots on different dates during the period between July, 2002, and May, 2003, show a reproducibility of <9% for Se and <5% for As. The detailed analytical procedure is essentially the same as that described by Robinson *et al.* (1998).

For S isotope analysis, laurite grains from Tambanio River were examined with a SEM-EDS without carbon coating and each grain (0.6 to 1.2 mg) was ground in an agate mortar together with V_2O_5 (1:3 weight ratio). The mixture containing ~0.05–0.59 mg of laurite was placed in tin foil and injected into a CE Elemental Analyzer. The samples were combusted at ~1700ºC to release SO_2. The SO_2 gas was introduced to a Finnigan-Mat Delta Plus mass spectrometer for the isotope analysis after passing through 7 ml of silica at ~1000ºC and Cu at ~600ºC to buffer O isotopes and reduce SO_3. Duplicate or triplicate analyses of all samples show a reproducibility of ±0.2‰. The standards used were: IAEA-S1 (–0.3‰) and IAES-S2 (+21.7‰).

The XRD analyses were carried out on crushed grains and analysed using a Rigaku position-sensitive detector microdiffraction goniometer (PSD-MDG) at 50 kV, 180 mA, scanned over the range 5–70º2θ.

Results

Morphology and mineralogy of grains

Most grains are sub-rounded to spherical with abundant pits and conchoidal fractures (Figs 2 and 3, Repository 1 and 2). Several grains form euhedral to subhedral crystals with evidence of abrasion on the crystal faces (Figs 2 and 3, Repository 1 and 2). There are no significant differences in the morphology of samples from Pontyn and Tambanio.

The XRD pattern confirmed that the grains are laurite. They contain substantial amounts of the OsS_2 component, ranging from 18 to 38%, up to 12% of the IrS_2 component, and minor (up to 1.2%) amounts of the PdS_2 component (Fig. 5, Table 1). The concentrations of Os, Ru and Ir are broadly correlated (Fig. 6); grains containing more Os show less Ir (correlation coefficient, r = 0.83) and Ru (r = 0.67). Samples from Tambanio River show a narrower spread than Pontyn samples. Tambanio samples plot the end-

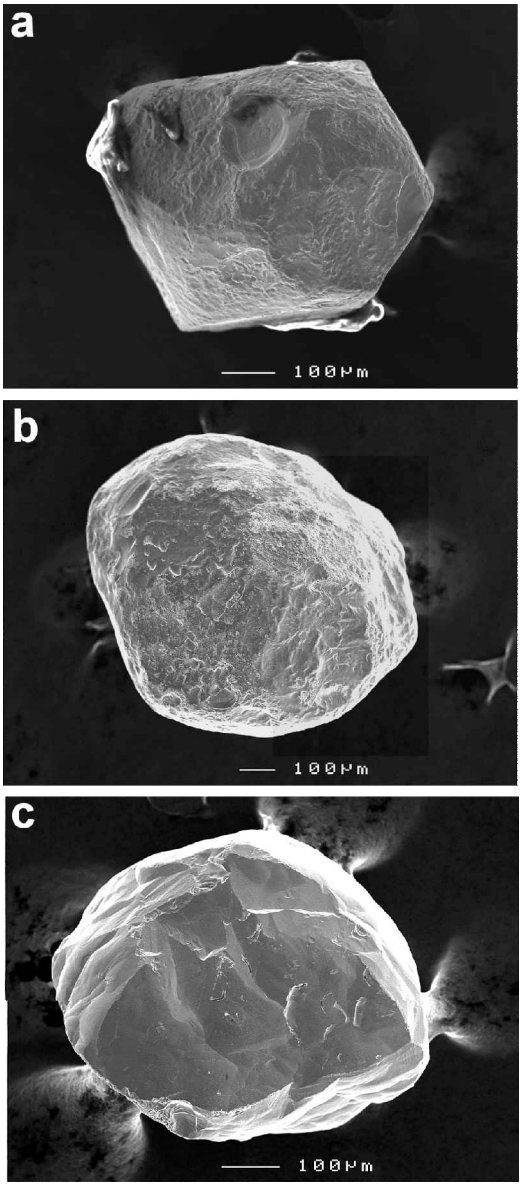

FIG. 3. Laurite grains used for the S isotope study listed in Table 3: (*a*) Gr-3; (*b*) Gr-4; (*c*) Gr-5.

member of the compositional variation with high Ir and Se and low Os and As (Fig. 6)

Laurite grains from Pontyn commonly show intra-compositional zoning due to different concentrations of Os and Ru (Figs 2*b*,*f* and 4*c*). The zoning patterns are not necessarily symmetrical. Some show inhomogeneity with diffuse boundaries without any growth bands (Repository R 1h (see the data section of the Mineralogical Society website: www.minersoc.org/pages/e_journals/dep_mat.htm)) and some show sharp boundaries between growth bands of different compositions (Fig. 2*b*,*f*). The growth pattern shows earlier Os-rich bands surrounded by Ru-rich rims (Figs 2*b* and 4*c*), but reverse zoning with exterior Os-rich growth bands is also observed (Fig. 2*f*). One grain shows several Os-rich interiors surrounded by Os-poor rims (Repository R 1n). Laurite grains from Tambanio are mostly homogeneous with no internal textures (Repository R 1q and R 1s).

There are grains with growth bands truncated by the external shape (Fig. 2*b*,*f*). The truncation of growth bands in crystals is commonly interpreted by later fragmentation of a once larger grain. This is possible for a grain that shows fracturing (Fig. 2*f*), but it is not applicable for all grains. For example, some grains show truncation of growth bands by a euhedral external shape (Fig. 2*b*). Such a growth pattern may be formed due to the nucleation and crystal growth of laurite in a limited space, or may be the result of fracturing in the sediments.

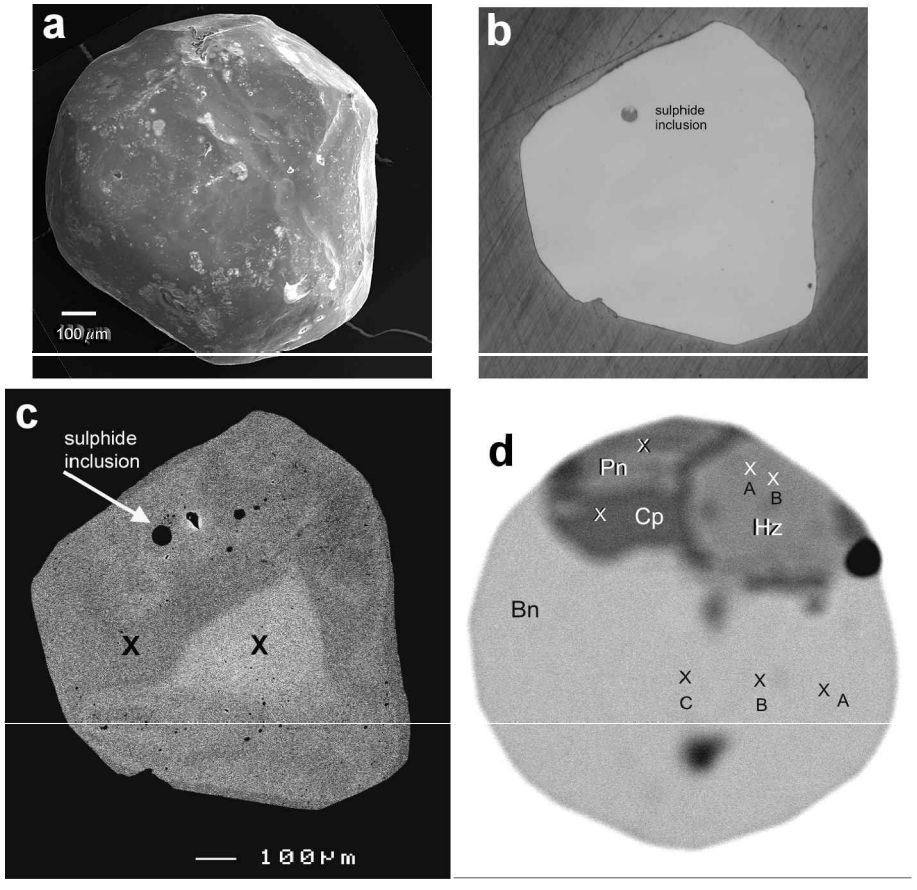

FIG. 4. Laurite grain, P-1-2, containing a sulphide inclusion: (*a*) Subhedral shape of the grain; (*b*) photomicrograph of the grain; (*c*) BSE electron image of the grain; and (*d*) BSE image of the sulphide inclusion. The compositions of the areas marked by X are listed in Table 2. Abbreviations: Bn = bornite, Cp = chalcopyrite, Hz = heazlewoodite, Pn = pentlandite.

TABLE 1. Chemical composition of laurite grains from Pontyn (P) and Tambanio (T).

Core/rim	P-1-1 C	P-1-1 R	P-1-2 C	P-1-2 R	P-1-3 C	P-1-3 R	P-2-1 C	P-2-1 R	P-2-2 C	P-2-2 R	P-2-3 C	P-2-3 R	P-2-4 C	P-2-4 R	P-2-5 C	P-2-5 R	P-2-6 C	P-2-6 R	P-2-7 C	P-2-7 R	P-2-8 C	P-2-8 R
Os (%)	26.86	27.97	25.30	22.34	30.64	31.47	22.31	22.35	24.53	24.09	29.12	29.21	28.01	28.75	26.70	26.50	23.26	23.34	28.35	27.91	21.69	22.27
Ir (%)	6.17	6.22	3.92	4.29	5.11	5.18	9.52	9.41	4.30	4.45	4.19	4.12	4.00	3.76	5.84	5.97	10.95	10.84	4.02	4.11	10.00	9.88
Pt (%)	0.00	0.00	0.00	0.05	0.00	0.00	0.00	0.00	0.05	0.00	0.03	0.00	0.00	0.02	0.00	0.03	0.18	0.00	0.00	0.00	0.01	0.12
Ru (%)	33.30	32.57	36.79	38.89	31.41	30.64	34.60	34.62	36.84	37.25	33.27	33.28	34.43	34.00	33.96	33.93	32.10	32.21	34.11	34.37	34.36	33.94
Rh (%)	0.05	0.06	0.00	0.00	0.00	0.00	0.03	0.04	0.00	0.00	0.10	0.00	0.00	0.00	0.06	0.06	0.38	0.45	0.00	0.00	0.31	0.37
Pd (%)	0.66	0.41	0.35	0.35	0.34	0.38	0.38	0.40	0.56	0.41	0.35	0.45	0.39	0.37	0.38	0.44	0.43	0.42	0.41	0.43	0.44	0.34
S (%)	32.45	32.22	33.18	33.68	31.92	31.75	32.70	32.68	33.20	33.25	32.33	32.34	32.59	32.47	32.52	32.53	32.19	32.23	32.53	32.58	32.70	32.62
As (ppm)	5050	5430	4640	4120	5840	5890	4610	5030	5190	5440	6320	6080	5910	6360	5460	5370	5180	5150	5820	6140	4900	4590
Se (ppm)	147	140	144	167	200	193	204	196	199	204	169	155	168	164	186	183	176	188	184	174	197	196
S/Se	2210	2300	2300	2020	1600	1650	1600	1670	1670	1630	1910	2090	1940	1980	1750	1780	1830	1710	1770	1870	1660	1660
As/S*10^5	1540	1670	1390	1210	1810	1830	1400	1520	1550	1620	1930	1860	1800	1940	1660	1640	1590	1580	1770	1863	1485	1394
Shape*	euh	euh	round	round	ang	ang	subh	subh	round	round	ang	ang	round	round	ang	ang	round	round	round	round	round	round
Photo**	F2a F2b	F2a F2b	F4c	F4c	R1a R1b	R1a R1b	R1c R1d	R1c R1d	R1e R1f	R1e R1f	R1g R1h	R1g R1h	R1j R1k	R1j R1k			F2c F2d	F2c F2d				

Table 1 (*cont.*)

Core/rim	P-2-9 C	P-2-9 R	P-2-10 C	P-2-10 R	P-2-11 C	P-2-11 R	P-2-12 C	P-2-12 R	P-2-12 R	T-3-1 C	T-3-1 R	T-3-2 C	T-3-2 R	T-3-3 C	T-3-3 R	T-3-4 C	T-3-4 R	T-3-5 C	T-3-5 R	T-3-6 C	T-3-6 R
Os (%)	26.95	29.38	20.27	20.69	27.70	28.23	33.87	35.38	33.05	23.68	23.52	22.88	23.04	21.93	22.36	24.36	23.96	20.77	20.99	17.71	17.81
Ir (%)	4.98	4.90	11.76	11.51	5.12	4.60	2.78	2.71	2.74	9.11	9.20	10.62	10.44	8.52	8.71	9.39	9.46	11.09	11.31	10.48	10.43
Pt (%)	0.00	0.00	0.00	0.00	0.00	0.03	0.00	0.11	0.00	0.00	0.00	0.00	0.01	0.01	0.00	0.04	0.06	0.00	0.00	0.00	0.00
Ru (%)	34.33	32.42	34.23	34.15	33.60	33.65	30.51	29.33	31.13	33.38	33.29	33.03	33.13	35.72	35.03	32.86	33.20	34.27	33.98	37.45	37.53
Rh (%)	0.14	0.12	0.20	0.16	0.09	0.00	0.01	0.03	0.10	0.48	0.62	0.15	0.12	0.03	0.12	0.21	0.14	0.32	0.30	0.00	0.03
Pd (%)	0.42	0.40	0.45	0.44	0.45	0.48	0.46	0.33	0.45	0.36	0.36	0.45	0.39	0.39	0.49	0.33	0.31	0.40	0.36	0.58	0.41
S (%)	32.62	32.16	32.68	32.65	32.43	32.46	31.68	31.37	31.85	32.50	32.51	32.38	32.37	32.96	32.83	32.32	32.37	32.69	32.61	33.42	33.38
As (ppm)	5620	6200	4200	4130	6130	5590	6970	7450	6870	4970	4990	4780	4930	4430	4710	4970	5020	4570	4550	3560	4030
Se (ppm)	185	199	211	208	170	186	157	151	175	186	177	206	213	196	201	175	180	192	204	232	242
S/Se	1760	1620	1550	1570	1910	1750	2020	2080	1820	1750	1840	1570	1520	1680	1630	1850	1800	1700	1600	1440	1380
As/S*10^5	1706	1904	1274	1256	1869	1705	2171	2340	2130	1516	1520	1463	1508	1334	1423	1523	1537	1385	1383	1059	1198
Shape*	ang	ang	subh	subh	subh	subh	semh	semh	semh	semh	ang	ang	round	round	subh	subh	subh	sph	sph	ang	ang
Photo	F2e F2f	F2e F2f					R1m R1n	R1m R1n	R1m R1n	R1p R1q	R1p R1q									R1r R1s	R1r R1s

Abbreviations: ang = angular due to fracturing, euh = euhedral, round = rounded due to extensive abrasion, sph = spherical with no recognized crystal faces, subh = subhedral with minor rounding along the edge of crystal faces and fracturing.

** Photo numbers starting with R are in the Repository (available from the Mineralogical Society website: www.minersoc.org/pages/e_journals/dep_mat.htm) and those with F are amongst the figures published here.

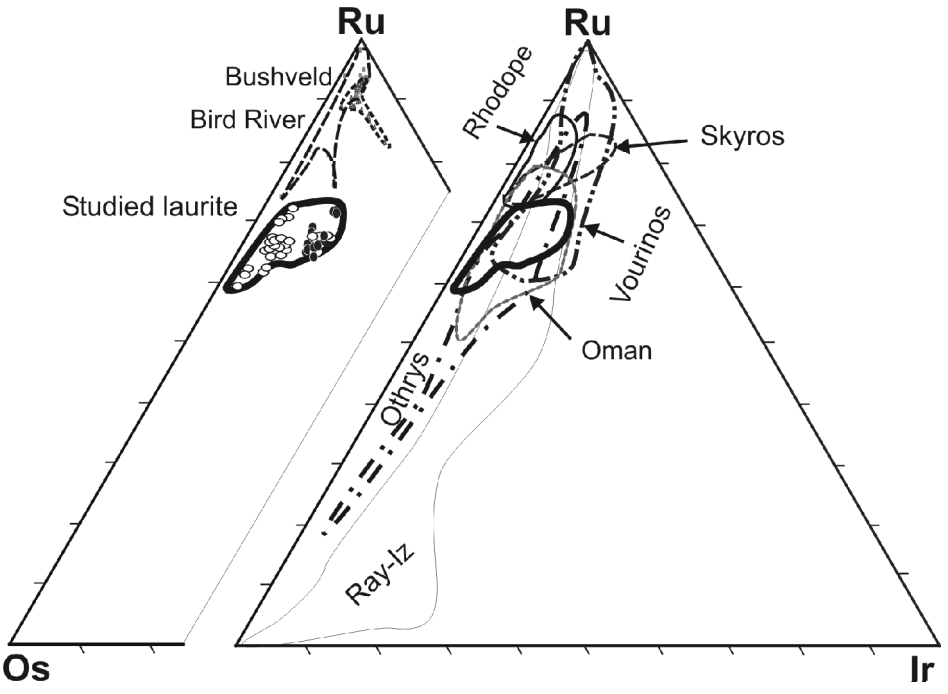

FIG. 5. Compositions of laurite plotted on the Ru-Ir-Os ternary. The compositions of the laurite studied (open circles for Pontyn samples, solid circles for Tambanio samples) are compared with those from the Bushveld layered igneous complex (South Africa) and Bird River Complex (Canada). The compositional fields of laurite from ophiolitic ultramafic complexes are shown on the right side of the ternary. They include Oman, Othrys (Greece), Skyros (Greece) and Vourinos (Greece), Ray-lz (Polar Ural, Russia), and Rhodope (Bulgaria). Data sources: Bird River (Cabri and Laflamme, 1988; Ohnenstetter *et al*., 1986), Bushveld (Schwellnus *et al*., 1976; Kingston and El-Dosuky, 1982), Oman (Ahmed and Arai, 2003); Othrys (Garuti *et al*., 1999*b*), Ray-Iz (Garuti *et al*., 1999*a*), Vourinos (Garuti and Zaccarini, 1997), Skyros (Tarkian *et al*., 1992), and Rhodope (Tarkian *et al*., 1991).

One grain contains a spherical inclusion of a mixture of chalcopyrite, bornite, pentlandite and heazlewoodite (Fig. 4). The texture between sulphide phases and the spherical outer shape (Fig. 4*d*) suggests that the inclusion was once homogeneous Fe-Cu-Ni sulphide and exsolved into monosulphide solid solution (mss) and intermediate sulphide solid solution (iss). Further crystallization formed pentlandite and heazlewoodite from mss and bornite and chalcopyrite from iss. Another grain contains several inclusions of Ca amphibole (Fig. 2*d*).

The crushed material from three grains gave a clean XRD pattern ascribed to laurite, with a cell edge a = 5.6117 Å. Taking an average composition of all laurites analysed (Table 1) gives $(Ru_{0.66}Os_{0.28}Ir_{0.06}Pd_{0.01})_{1.01}S_{2.00}$, which may be compared to 5.6089 Å, reported for laurite from Senduma Chrome Mines, Sierra Leone, with a more Ru-rich composition of $(Ru_{0.84}Os_{0.04}Ir_{0.04})_{0.95}S_{1.05}$ (Bowles *et al*., 1983).

Arsenic and selenium

All grains contain considerable amounts of Se and As, far greater than the detection limits of 15 and 370 ppm, respectively. The concentrations of Ir show a broad negative correlation with As (r = 0.77; Fig. 6*a*) and positive correlation with Os (r = 0.83; Fig. 6*b*). The As and Se contents show a broad negative correlation (r = 0.57; Fig. 6*c*). Grains with greater Os contain less Ir (Fig. 6*b*) and Se (Fig. 6*a*,*c*) and more As (r = 0.94; Fig. 6*d*). As mentioned above, the samples from Tambanio plot close to the end-member composition with high Ir and Se, and low Os and As.

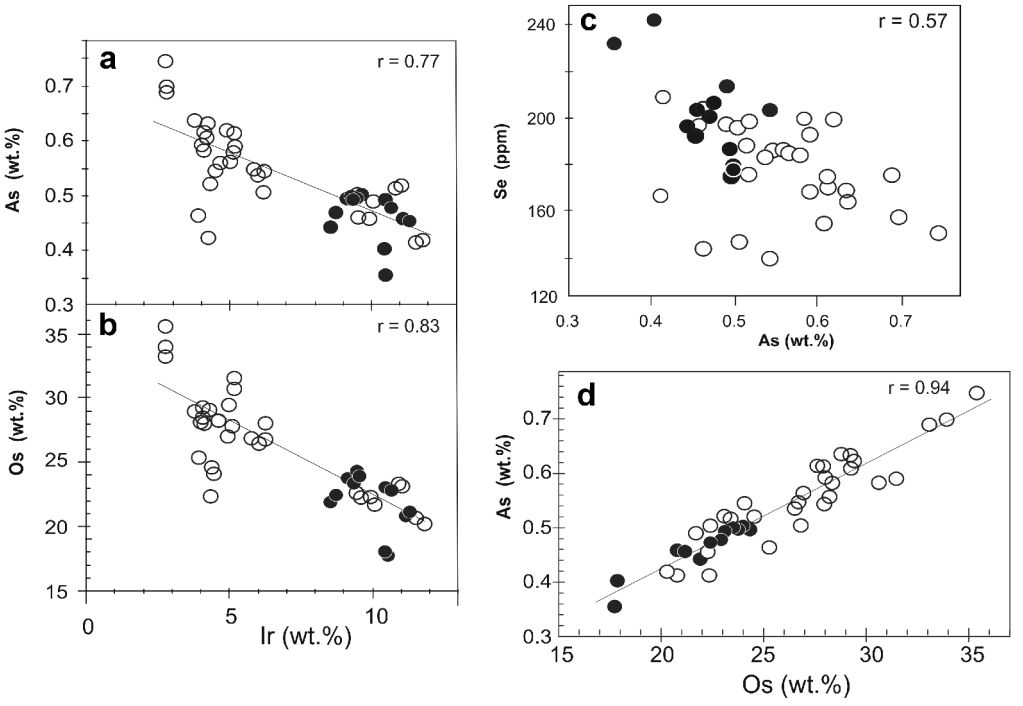

FIG. 6. Compositional variations of laurite grains, Ir *vs.* As and Ir *vs.* Os. Lines of calculated correlation and correlation coefficients, r, are shown. Open circles = Pontyn samples, solid circles = Tambanio samples. (*a*) Iridium *vs.* As, (*b*) Iridium *vs.* Os, (*c*) Arsenic *vs.* Se, (*d*) Osmium *vs.* As.

The S/Se ratios of laurite show a narrow spread between 1380 and 2300 (Table 1). The concentrations of Se in the sulphide inclusion show a considerable variation among different phases, with S/Se ratios varying from 3500 to 6560, but the concentrations are overall lower than the host laurite (Table 2). The weighted ratio of As/S of the sulphide inclusion is 38×10^{-5}, which is far lower than those of the host laurite, $>1000 \times 10^{-5}$. The data suggest that laurite incorporates As and Se in preference to base metal sulphides.

Sulphur isotopic compositions

The samples from Tambanio are homogeneous and free of inclusions. Thus, they were selected for S isotopic analysis. The values of all grains show a narrow spread in $\delta^{34}S$ values (+1.16±0.36‰) and minor enrichment of ^{34}S, but they are very close to the meteorite standard value of 0‰. The values are independent of the morphology and the composition of the grains (Table 3).

TABLE 2. Arsenic and selenium concentrations of sulphide inclusions in laurite and of laurite (ppm) (sample P-1-2, shown in Fig. 4)

		Se	As	S/Se	As/S × 10^5
Hz	Ni_3S_2	101	278	3500	79
Hz	Ni_3S_2	101	354	3500	100
Pn	$(Fe,Ni)_9S_8$	80	431	4150	130
Cp	$CuFeS_2$	56	262	6230	75
Bn	Cu_5FeS_4	41	37	6230	15
Bn		41	79	6230	31
Bn		39	67	6560	26
Laurite		194	4110	1810	1170
Laurite		188	4870	1870	1390
Laurite		194	4720	1810	1340
Laurite		182	5440	1930	1550
Laurite		170	5400	2070	1540
Laurite		179	5210	1970	1480

The area for the analysis is shown in Fig. 4*d*
Bo = bornite, Cp = chalcopyrite, Hz = heazlewoodite, Pn = pentlandite

TABLE 3. Sulphur isotope compositions of laurite grains.

Grain	Photograph*	Shape	Weight (μg)	$\delta^{34}S_{CD}$ (‰)
Gr-1	R 2a	Rounded with barely recognized crystal faces	269	+1.3
ditto			373	+1.1
Gr-2	R 2b	Rounded	135	+1.0
Gr-3	F 3a	Euhedral with pits	213	+1.8
ditto	ditto		230	+1.7
Gr-4	F 3b	Spherical	399	+1.2
ditto	ditto		408	+1.3
ditto	ditto		383	+1.4
Gr-5	F 3c	Extensively fractured	110	+1.2
ditto	ditto		164	+1.7
Gr-6	R 2c	Subhedral with abundant pits	235	+1.2
ditto	ditto		234	+1.3
Gr-7	R 2d	Subhedral, fractured	212	+0.5
ditto	ditto		269	+0.5
ditto	ditto		360	+0.8
Gr-8	R 2e	Well rounded	89	+1.1
ditto	ditto		98	+1.0
ditto	ditto		186	+1.2
Gr-10	not shown	Rounded	406	+1.4
Gr-11	R 2f	high Ru, rounded	299	+1.2
ditto	not shown		590	+1.3
Gr-12	R 2g	Euhedral with abundant abrasion pits	391	+1.0
ditto	ditto		373	+1.1
Gr-13	R 2h	Angular, fractured	50	+0.5
Gr-14	not shown	Rounded	840	+0.8

* numbers starting with R are in the Repository, (available from the Mineralogical Society website: www.minersoc.org/pages/e_journals/dep_mat.htm) and those with F are amongst the figures published here.

Discussion

Origin of the host rocks

The origin of Alpine-type ultramafic intrusions is controversial, with two principal opinions: they are obducted slices of oceanic upper mantle, or cumulates of mafic magma in supra-subduction zones (e.g. Robertson, 2002). The latter magmas form by high degrees of partial melting in a refractory mantle. Ruthenium and Os are both refractory, Ir-type PGE and are concentrated in the residual mantle (e.g. Guillot *et al.*, 2000); thus laurite is common in refractory mantle rocks and cumulates of melt formed from such a refractory mantle. This is confirmed by several mineralogical studies of PGM from Alpine-type ultramafic intrusions and refractory mantle rocks (e.g. Melcher *et al.*, 1997; Garuti *et al.*, 1999*a*). Thus, the major-element compositions of the laurites from Pontyn and Tambanio Rivers are consistent with their crystallization in the upper refractory mantle or cumulates of mafic magmas that originated from a refractory mantle.

Sulphur isotopic compositions

Sulphide formation in surface environments requires the reduction of dissolved sulphate. This reduction of sulphate, either by a kinetic or equilibrium process, at low temperature is accompanied by large isotopic fractionation and the product, S^{2-}, has low $\delta^{34}S$, as much as 60‰ less than SO_4^{2-}values (e.g. Hoefs, 1997). In addition, dissimilatory sulphate-reducing bacteria, which probably participate in sulphate reduction in surface environments, produce S^{2-} with variable isotopic compositions because bacterial reduction is affected by many factors, such as nutrient for

TABLE 4. Compositional characteristics of sulphide formed under different environments.

	Mantle-derived magmatic source	Upper-crust hydrothermal	Sedimentary sulphide
$\delta^{34}S$	Consistent, ~0‰	May vary	Highly variable
S/Se	Consistent, $\leqslant$ 3000	May vary	Very high

bacteria, sulphate concentrations and bacterial population. Hence, sulphides formed near the surface show a large variation in $\delta^{34}S$, as shown in many sedimentary rocks (Table 4). Our data thus rule out laurite formation in near-surface environments, including "element agglutination" (Augustithis, 1965) or "accretion" of fine particles (Cousins, 1973; Cousins and Kinloch, 1976) during weathering and deposition of placers (Bowles, 1986, 1988; Barker and Lamal, 1989).

Sulphur isotopic fractionation between oxidized and reduced S species becomes smaller at higher temperatures, but is still significant. Thus, sulphides formed at high temperatures, even ~500ºC, may show a significant isotopic variation when they form from fluids containing significant sulphate (e.g. Cameron and Hattori, 1987). However, isotopic fractionation among reduced S species is small at high temperature. Ripley *et al.* (2003) show that the variation in $\delta^{34}S$ is <2‰, even after extensive degassing at magmatic temperatures. Therefore, the consistent S isotopic compositions, near meteoritic sulphur values of 0‰, from the laurite samples studied indicate that their formation did not involve any oxidation-reduction of sulphide sulphur. Thus, the laurite formed under reduced conditions at deep levels in the crust or mantle (Table 4).

Compositional variations

Laurite belongs to the isometric diploidal system, similar to pyrite. Pyrite and laurite contain divalent metals (Fe^{2+}, Ru^{2+}, Os^{2+}, Ir^{2+}) and two covalently bonded sulphur atoms as a dianion. Pyrite can accommodate significant amounts of As, and most of the As replaces S, forming $(As\text{-}S)^{2-}$ (Fleet *et al.*, 1993). Pyrite with high concentrations of As may contain thin, 10 to 15 Å, layers of arsenopyrite-like structure (Simon *et al.*, 1999). Irarsite (IrAsS) and ruarsite (RuAsS) belong to this arsenopyrite group with a crystal configuration similar to that of arsenopyrite.

The correlation between As and Se is, therefore, easily understood, considering that both elements occupy the S site, forming $(As\text{-}S)^{2-}$ and $(Se\text{-}S)^{2-}$. There are fewer S atoms in As-rich laurite. In addition, anion pairs of $(Se\text{-}As)^{2-}$ may not be easily formed in the structure.

The laurite samples studied also display correlations among metal ions. The atomic ratio of Os to Ir is 1.2, which suggests the two heavy atoms are nearly substituting for each other. However, the atomic ratios of Ir/As and As/Se are 18 and 71, respectively. This means that the loss of 18 atoms of Ir corresponds to an increase of 1 atom of As and 71 atoms of As to 1 atom of Se. The observed compositional variations may be attributed to either crystallographic effects or compositional control of the environment for crystal growth.

We suggest the latter. First, the correlations between Os and Ir and between Ir and As are not easily explained by the crystallographic configuration, because these three metals form divalent cations. In addition, Ru and Os should be interchangeable in the crystal considering that the two have very similar ionic radii and electronegativities. Thus, high Ir concentrations in low-Os laurite are attributed to an external cause, the compositional variation of rocks where the laurite grains crystallized. Our proposed interpretation is further supported by the compositions of laurite from other locations (Figs 7 and 8). For example, laurite from the Bushveld Complex shows a wide range of Ir almost independent of Os content (Fig. 7), but a broad positive correlation between Ir and As (Fig. 8). Considerable compositional variation in a single sample is also noted in the western Bushveld Complex (Maier *et al.*, 1999). Laurite grains from other ophiolitic rocks also show a wide scatter without any apparent correlations on the diagrams of Os *vs.* Ir and Ir *vs.* As (Fig. 8).

Selenium concentration among different sulphides

The S/Se ratios of laurite are much lower than those in the sulphide inclusion. Furthermore, different phases in the inclusion show a wide

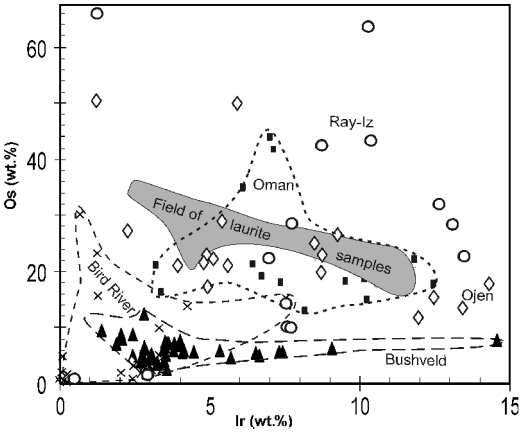

FIG. 7. Ir and Os contents of laurite compared to those from the Merensky Reef of the Bushveld Complex (solid triangles), Bird River complex (X), Ray-Iz (open circles), Ojen in Ronda Complex (open diamonds), and Oman (solid squares). The data from Ojen are from Torres-Ruiz *et al*. (1996). The other data sources are listed in Fig. 5.

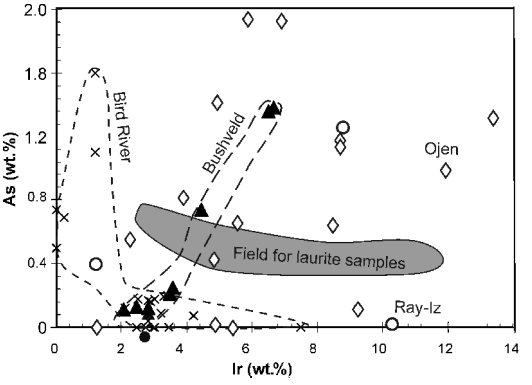

FIG. 8. Ir and As contents of laurite compared to those from other locations. Data sources are listed in Fig. 5.

variation, chalcopyrite has the highest S/Se ratio, 7350, and heazlewoodite the lowest ratio, ~3500. The weighted average value of S/Se is calculated to be 5890 using 82.7 vol.% for bornite, 6.0 vol.% for pentlandite, 11.0 vol.% for heazlewoodite, 0.24 vol.% for chalcopyrite. The volume of each phase was calculated after the measurement of surface area on a digital photograph using the 'Image J' computer program.

$$(Ru,Os)Se_2 + (Cu\text{-}Fe\text{-}Ni)S_2 = (Ru,Os)S_2 + (Cu\text{-}Fe\text{-}Ni)Se_2$$

The apparent distribution coefficient for Se, K_{Se}, is ~3.0. The value is large, probably due to low-temperature re-equilibration, considering the rapid diffusion of Se in sulphides (e.g. Bethke and Barton, 1971). Nevertheless, the data suggest that laurite preferentially incorporates Se compared to base metal sulphides.

Variations of S/Se ratios

Surface waters contain very low Se (i.e. high S/Se ratios) because of the sluggish oxidation of Se. This is reflected by low Se in sulphides in most clastic sedimentary rocks, evaporites and seawater, S/Se > 100,000 (Measures and Burton, 1980; Fig. 9). Selenium may be enriched in Fe-oxide chemical sediments due to strong adsorption of SeO_3^{2-} on an oxide surface and may also be enriched in organic-rich black shales formed in anoxic basins (e.g. Stanton, 1972; Howard, 1977), but these cases are not applicable to the studied samples. Thus, the S/Se data from the laurite grains studied are not consistent with their formation in surface environments (Table 4).

The values of S/Se in laurite are even lower than that of the primitive mantle (3300; McDonough and Sun, 1995) and those for the mid-oceanic ridge basalts (3000–6000; Hamlyn and Keays, 1986; Peach *et al*., 1990). Instead, the values are comparable to those of mantle sulphides that originated from sub-arc mantle wedges (Hattori *et al*., 2002). Selenium and S show a similar geochemical behaviour. The

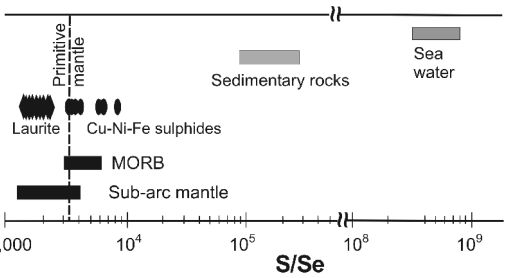

FIG. 9. S/Se ratios of the samples studied (laurite and Cu-Ni-Fe sulphides) compared to the values for the primitive mantle, sulphides from sub-arc mantle, mid-oceanic ridge basalts, and sedimentary rocks. Data sources: primitive mantle (McDonough and Sun, 1995), sulphides from sub-arc mantle (Hattori *et al*., 2002), mid-oceanic ridge basalts (Hamlyn and Keays, 1986; Peach *et al*., 1990), sedimentary rocks (Stanton, 1972; Leutwein, 1978) and seawater (Measures and Burton, 1980).

causes of fractionation include: (1) redox change (Yamamoto, 1976); (2) contribution of Se-poor surface waters; and (3) the formation of other phases (e.g. Bethke and Barton, 1971).

(1) Selenium and S are fractionated in solutions near the redox boundary of S. When S is oxidized to form SO_4^{2-} and HSO_4^-, Se remains as H_2Se, HSe^- and Se^{2-}. Thus, the S^{2-}/Se^{2-} ratios in solutions near the redox boundary of sulphur vary widely due to oxidation of S. Sulphides formed from such solutions show a large variation in S/Se ratio. This is not applicable for the studied samples because the sulphur isotopic data indicate no redox change of S.

(2) Incursion of surface waters may cause a large variation of S/Se ratios because surface waters show very high S/Se ratios due to sluggish oxidation of Se. For example, seawater shows ratios $> 4 \times 10^8$ (e.g. Measures and Burton, 1980).

(3) The remaining possibility is the removal of different sulphide phases and melt. Laurite preferentially incorporates Se compared to base-metal sulphides, as shown in the fractionation of Se among sulphide grains. Ruthenium and Os are considered to be refractory metals, retained in the mantle during partial melting. In contrast, Cu and Fe are incompatible with mantle minerals and are preferentially removed from the mantle during partial melting. Thus, partial melting and removal of base metal sulphides would lead to the enrichment of Se (lower S/Se) in the mantle. This is further supported by low S/Se ratios of sulphides found in refractory mantle underlying arcs (Hattori *et al.*, 2002). Low S/Se ratios of the studied laurite samples, therefore, probably reflect the origin of S in laurite from a refractory mantle. We, therefore, suggest that the laurite grains crystallized either in the upper refractory mantle or in the cumulates of mafic magmas that were derived from such a refractory mantle.

The proposed interpretation implies high-temperature crystallization of laurite and this is consistent with experimental data on the stability of laurite (Andrews and Brenan, 2002).

Conclusions

The studied laurite grains from placers in southern Kalimantan show a major element composition similar to laurite grains found in ophiolitic ultramafic rocks of other regions. Furthermore, the S/Se ratios of laurite show a narrow range, and with lower values than base metal sulphides. The ratios are similar to those of sulphides from the refractory mantle wedge, suggesting that the laurite grains crystallized in the refractory upper mantle or in cumulate ultramafic rocks of magmas originated from such a refractory mantle. The evidence suggests that the emplacement of laurite-bearing ultramafic rocks in the upper crust was followed by erosion, which liberated the laurite grains to be concentrated in placers.

Values of $\delta^{34}S$ for all PGM studied are similar, near 0‰. The consistent S isotopic values near chondritic composition discount their crystallization at moderate to low temperatures at shallow crustal levels. Instead, they formed at depth where S has not undergone redox changes.

Acknowledgements

We are pleased to be able to contribute this paper in the memory of Alan J. Criddle of the Natural History Museum, London, who made numerous contributions to the subject of ore microscopy, and who was a good friend of the second author.

We thank Alan Hart, Natural History Museum, London, for the laurite grains from the type locality (Pontyn River), Monika Wilke-Alemany for sample preparation in the laboratory, Paul Middlestead and Wendy Abdi, the University of Ottawa, for maintenance of the mass spectrometry laboratory, and Peter Jones and Lew Ling, Carleton University, for assisting with the SEM and electron probe analysis, and to John Wilson, CANMET/MMSL for the XRD analysis. We are also grateful to Ernst A.J. Burke of Vrije University for the information on the occurrence of the Pontyn laurite, Chris Stanley, Natural History Museum, London, for sending us a polished section containing PGM from Rio Pilpe, Colombia, that he and Alan Criddle had studied, even though it was not used in this study. LJC acknowledges the technical support provided by CANMET during his tenure as Emeritus Research Scientist. This project was funded by a NSERC grant to KHH. Comments by A. Bookstrom and S. Box, USGS, and by journal reviewers Baruch Spiro and Adrian Boyce helped to improve the manuscript.

References

Ahmed, A.H. and Arai, S. (2003) Platinum-group minerals in podiform chromitites of the Oman ophiolite. *The Canadian Mineralogist*, **41**, 597–616.

Andrews, D. and Brenan, J.M. (2002) Phase equilibrium constraints on the magmatic origin of laurite +Ru-Os-

Is alloy. *The Canadian Mineralogist*, **40**, 1705–1716.

Augustithis, S.S. (1965) Mineralogical and geochemical studies of the platiniferous dunite-birbirite-pyroxenite complex of Yubdo, Birbir, W. Ethiopia. *Chemie der Erde*, **24**, 159–196.

Barker, J.C. and Lamal, K. (1989) Offshore extension of platiniferous bedrock and associated sedimentation of the Goodnews Bay ultramafic complex, Alaska. *Marine Mining*, **8**, 365–390

Bethke, P.M. and Barton, P.B., Jr. (1971) Distribution of some minor elements between coexisting sulfide minerals. *Economic Geology*, **66**, 140–163.

Bird, J.M., Meibom, A., Frei, R. and Nägler, T.F. (1999) Osmium and lead isotopes of rare OsIrRu minerals derivation from the core-mantle boundary region? *Earth and Planetary Science Letters*, **170**, 83–92.

Bowles, J.F.W. (1986) The development of platinum-group minerals in laterites. *Economic Geology*, **81**, 1278–1285.

Bowles, J.F.W. (1988) Further studies of the development of platinum-group minerals in the laterites of the Freetown layered complex, Sierra Leone. Pp. 273–280 in: *Geo-Platinum '87* (H.M. Prichard, P.J. Potts, J.F.W. Bowles and S.J. Cribb, editors). Elsevier Applied Science, New York.

Bowles, J.F.W, Atkin, D., Lambert, J.L.M., Deans, T. and Phillips, R. (1983) The chemistry, reflectance, and cell size of the erlichmanite (OsS_2)–laurite (RuS_2) series. *Mineralogical Magazine*, **47**, 465–471.

Bowles, J.F.W., Lyon, I.C., Saxton, J.M. and Vaughan, D.J. (2000) The origin of platinum group minerals from the Freetown intrusion, Sierra Leone, inferred from osmium isotope systematics. *Economic Geology*, **95**, 539–548.

Burgath, K.-P. (1988) Platinum-group minerals in ophiolitic chromitites and alluvial placer deposits, Meratus-Bobaris area, southeast Kalimantan. Pp. 383–403 in: *Geo-Platinum '87* (H.M. Prichard, P.J. Potts, J.F.W. Bowles and S.J. Cribb, editors). Elsevier Applied Science, New York.

Burgath, K.P. and Mohr, M. (1986) Chromitites and platinum-group minerals in the Meratus-Bobaris ophiolite zone, south-east Borneo. Pp. 333–349 in: *Metallogeny of Basic and Ultrabasic Rocks* (M.J. Gallagher, R.A. Ixer, C.R. Neary and H.M. Prichard, editors). The Institution of Mining and Metallurgy, London.

Cabri, L.J. and Laflamme, J.H.G. (1988) *Mineralogical study of the platinum-group element distribution and associated minerals from three stratigraphic layers, Bird River Sill, Manitoba*. CANMET Report CM 88-1E, 52 pp.

Cabri, L.J. and Harris, D.C. (1975) Zoning in Os-Ir alloys and the relation of the geological and tectonic environment of the source rocks to the bulk Pd:Pt+Ir+Os ratio for placers. *The Canadian Mineralogist*, **13**, 266–274.

Cabri, L.J., Harris, D.C. and Weiser, T.W. (1996) The mineralogy and distribution of platinum-group mineral (PGM) placer deposits of the world. *Exploration and Mining Geology*, **5**, 73–167.

Cameron, E.M. and Hattori, K. (1987) Archaean gold mineralization and oxidized hydrothermal fluids. *Economic Geology*, **82**, 1177–1191.

Cousins, C.A. (1973) Notes on the geochemistry of the platinum-group elements. *Transactions, Geological Society of South Africa*, **76**, 77–81.

Cousins, C.A. and Kinloch, E.D. (1976) Some observation on textures and inclusions in alluvial platinoids. *Economic Geology*, **71**, 1377–1398

Fleet, M.E., Chryssoulis, S.L., MacLean, P.J., Davidson, R. and Weisener, C.G. (1993) Arsenian pyrite from gold deposits: Au and As distribution investigated by SIMS and EMP, and color staining and surface oxidation by XPS and LIMS. *The Canadian Mineralogist*, **31**, 1–17.

Garuti, G. and Zaccarini, F. (1997) In-situ alteration of platinum-group minerals at low temperature: evidence from serpentinized and weathered chromitites of the Vourinos complex (Greece). *The Canadian Mineralogist*, **35**, 611–626.

Garuti, G., Zaccarini, F., Moloshag, V. and Alimov, V. (1999*a*) Platinum-group minerals as indicators of sulfur fugacity in ophiolitic upper mantle: An example from chromitites of the Ray-Iz ultramafic complex, Polar Urals, Russia. *The Canadian Mineralogist*, **37**, 1099–1115.

Garuti, G., Zaccarini, F. and Economou-Eliopoulos, M. (1999*b*) Paragenesis and composition of laurite from chromitites of Othrys (Greece). Implications for Os-Ru fractionation in ophiolitic upper mantle of the Balkan Peninsula. *Mineralium Deposita*, **34**, 312–319.

Guillot, S., Hattori, K.H. and de Sigoyer, J. (2000) Mantle wedge serpentinization and exhumation of eclogites: Insights from eastern Ladakh, NW Himalaya. *Geology*, **28**, 199–202.

Hamlyn, P.R. and Keays, R.R. (1986) Sulfur saturation and second-stage melts: Application to the Bushveld platinum metal deposits. *Economic Geology*, **81**, 1431–1445.

Hattori, K. and Cabri, L.J. (1992) Origin of platinum group mineral nuggets inferred from osmium-isotope study. *The Canadian Mineralogist*, **30**, 289–301.

Hattori, K., Cabri, L.J. and Hart, S.R. (1991) Osmium isotope ratios of PGM nuggets associated with the Freetown Layered Complex, Sierra Leone, and their origin. *Contributions to Mineralogy and Petrology*, **109**,10–18.

Hattori, K. Burgath, K.-P. and Hart, S.R. (1992) Os-isotope study of platinum-group minerals in

chromitites in alpine-type ultramafic intrusions and the associated placers in Borneo. *Mineralogical Magazine*, **56**, 156–164

Hattori, K.H., Arai, S. and Clarke, D.B. (2002) Selenium, tellurium, arsenic and antimony contents in primary mantle sulfides. *The Canadian Mineralogist*, **40**, 637–650.

Hoefs, J. (1997) *Stable Isotope Geochemistry*, 4th edition. Springer, New York, 201 pp.

Howard, J.H., III (1977) Geochemistry of selenium: formation of ferroselite and selenium behavior in the vicinity of oxidizing sulfide and uranium deposits. *Geochimica et Cosmochimica Acta*, **41**, 1665–1678.

Johan, Z., Slansky, E. and Kelly, D.A. (2000) Platinum nuggets from the Kompiam area, Enga Province, Papua New Guinea: evidence for an Alaskan-type complex. *Mineralogy and Petrology*, **68**, 159–176.

Kingston, G.A. and El-Dosuky, B.T. (1982) A contribution on the platinum-group mineralogy of the Merensky Reef at the Rustenburg Platinum Mine. *Economic Geology*, **77**, 1367–1384.

Leutwein, F. (1978) Selenium. Abundance in common sediments and sedimentary rock types. Pp. 34-K-1–34-K-4 in: *Handbook of Geochemistry*, vol. 2/3 (K.H. Wedepohl, editor). Springer-Verlag, Berlin.

Maier, W.D., Prichard, H.M., Barnes, S.J. and Fisher, P.C. (1999) Compositional variation of laurite at Union Section in the Western Bushveld Complex. *South African Journal of Geology*, **102**, 286–292.

McDonough, W.F. and Sun, S.-S. (1995) The composition of the Earth. *Chemical Geology*, **120**, 223–253.

Measures, C.I. and Burton, J.D. (1980) The vertical distribution and oxidation states of dissolved selenium in the Northeast Atlantic ocean and their relationship to Biological Processes. *Earth and Planetary Science Letters*, **46**, 385–396.

Meibom, A., Sleep, N.H., Chamberlain, C.P., Coleman, R.G., Frey, R., Hren, M.T. and Wooden, J.L. (2002) Re-Os isotopic evidence for long-lived heterogeneity and equilibration processes in the Earth's upper mantle. *Nature*, **419**, 705–708.

Melcher, F., Grum, W., Simon, G., Thalhammer, T.V. and Stumpfl, E.F. (1997) Petrogenesis of the ophiolitic giant chromite deposits of Kempirsai, Kazakhstan: a study of solid and fluid inclusions in chromite. *Journal of Petrology*, **38**, 1419–1458.

Ohnenstetter, D., Watkinson, D.H., Jones, P.C. and Talkington, R. (1986) Cryptic compositional variation in laurite and enclosing chromite from the Bird River Sill, Manitoba. *Economic Geology*, **81**, 1159–1168.

Ottemann, J. and Augustithis, S.S (1967) Geochemistry and origin of "platinum-nuggets" in lateritic covers from ultrabasic rocks and Birbirites of W. Ethiopia. *Mineralium Deposita*, **1**, 269–277.

Peach, C.L., Mathez, E.A. and Keays, R.R. (1990) Sulfide melt-silicate melt distribution coefficients for noble metals and other chalcophile elements as deduced from MORB: Implications for partial melting. *Geochimica et Cosmochimica Acta*, **54**, 3379–3389.

Ripley, E.M., Lightfoot, P.C., Li, C. and Elswick, E.R. (2003) Sulfur isotopic studies of continental flood basalts in the Noril'sk region: Implications for the assoiciation between lavas and ore-bearing intrusions. *Geochimica et Cosmochimica Acta*, **67**, 2805–2817.

Robertson, A.H.F. (2002) Overview of the genesis and emplacement of Mesozoic ophiolites in the Eastern Mediterranean Tethyan region. *Lithos*, **65**, 1–67.

Robinson, B.W., Ware, N.G. and Smith, D.G.W. (1998) Modern electron-microprobe trace-element analysis in mineralogy. Pp. 153–180 in: *Modern Approaches to Ore and Environmental Mineralogy* (L.J. Cabri and D.J. Vaughan, editors). Mineralogical Association of Canada, Short Course Volume **27**, Ottawa.

Schwellnus, J.S.I., Hiemstra, S.A. and Gasparrini, E. (1976) The Merensky reef at the Atok platinum mine and its environs. *Economic Geology*, **71**, 249–260.

Simon, G., Huang, H., Penner-Hahn, J.E., Kesler, S.E. and Kao, L.S. (1999) Oxidation state of gold and arsenic in gold-bearing arsenian pyrite. *American Mineralogist*, **84**, 1071–1079.

Slansky, E., Johan, Z., Ohnenstetter, M., Barron, L.M. and Suppel, D. (1991) Platinum mineralization in the Alaskan-type intrusive complexes near Fifield, N.S.W., Australia. Part 2. Platinum-group minerals in placer deposits at Fifield. *Mineralogy and Petrology*, **43**,161–180.

Stanton, R.L. (1972) *Ore Petrology*. McGraw-Hill Book Company, New York, 713 pp.

Stumpfl, E.F. (1974) The genesis of platinum deposits: Further thoughts. *Minerals Science* and *Engineering*, **6**, 120–141.

Tarkian, M., Naidenova, E. and Zhelwaskova-Panayotova, M. (1991) Platinum-group minerals in chromitites from the Eastern Rhodope ultramafic complex, Bulgaria. *Mineralogy and Petrology*, **44**, 73–87.

Tarkian, M., Economou-Eliopoulos, M. and Eliopoulos, D.G. (1992) Platinum group minerals and tetraauricupride in ophiolitic rocks of Skyros Island, Greece. *Mineralogy and Petrology*, **47**, 55–66.

Torres-Ruiz, J., Garuti, G., Gazzotti, M., Gervilla, F. and Hach-Ali, P.F. (1996) Platinum-group minerals in chromitites from the Ojen lherzolite massif (Serrania de Ronda, Betic, Cordillera, Southern Spain). *Mineralogy and Petrology*, **56**, 25–50.

Wöhler, F. (1866) Ueber ein neues Mineral von Borneo: Laurit. *Königliche Gesellschaft der Wissenschaften zu Göttingen, Nachrichten*, 155–160.

Yamamoto, M. (1976) Relationship between Se/S and sulfur istope ratios of hydrothermal sulfide minerals. *Mineralium Deposita*, **11**, 197–209.

Zientek, M.L. and Page, N.J. (1990) *Consultancy services in platinum-group mineral exploration for the Directorate of Mineral Resources*. Contract No. 569/PIO/ADB/1988, US Geological Survey Open-File Report 90-527, 326 pp.

Zientek, M.L., Pardiartom, B., Simandjuntak, H.R.W., Wikrama, A., Oscarson, R.L., Meier, A.L. and Carlson, R.R. (1992) Placer and lode platinum-group minerals in South Kalimantan, Indonesia; evidence for derivation from Alaskan-type ultramafic intrusions. *Australian Journal of Earth Sciences*, **39**, 405–417.

[*Manuscript received 4 August 2003: revised 13 January 2004*]